

Impact of Rain Attenuation in Borneo using Free Space Optics Propagation

Tauffiq Khirham¹, AK Rahman¹, Sahari S.K¹, Zamhari N¹, Tamrin F.K², S A Aljunid³, N Ali³ and R Endut³

¹ Department of Electrical & Electronics, University Malaysia Sarawak, Kuching, Malaysia

² Department of Mechanical, University Malaysia Sarawak, Kuching, Malaysia

³ Faculty of Electronic Engineering Technology (FTKEN), University Malaysia Perlis, Pauh Putra Campus, 02600 Arau, Perlis, Malaysia

ABSTRACT

In recent years, Free Space Optics (FSO) communication provides attractive bandwidth enhancement with unlicensed bands worldwide spectrum. However, the link capacity and availability are the major concern in the different atmospheric conditions. The reliability of the link is highly dependent on weather conditions that attenuate the signal strength. In the tropical region specifically in Borneo Sarawak, rain is the dominant weather that act as the limiting factor to FSO performance. Hence, this study highlights on the impact of rain attenuation to the performance of FSO communication system. The finding is based on atmospheric model and performed through the simulation of OptiSystem software. The design of parameters in the simulation involves iteration of wavelengths, size of transmitter and receiver aperture and beam divergence angle. The simulation result shows longer wavelength 1550nm is much better than 785nm. The 0.25m of receiver aperture and transmitter aperture at 0.05m can reduce the loss. Narrow beam divergence angle can reduce the power consumption and maintain the high power at receiver. The analysis indicates that proposed FSO communication system is capable to withstand the attenuation from rain weather.

Keywords: Free Space Optics, atmospheric model, OptiSystem, aperture, beam divergence

1. INTRODUCTION

Optical wireless communications are based on the data transmission through the atmosphere using optical carriers. Optical links can be very short in range (in the order of cm), as well as long range (hundreds of km). Hence, the terms free-space optic or well known as FSO typically refer to outdoor terrestrial links operating over distances from a few tens of meters up to several kilometers. The use of FSO is highly recommended in the telecommunication community for applications that demand capability of very large bandwidth. The advantages of FSO communication system over conventional fiber and microwave links are low costs of equipment, flexible and license-free installation [1]. The propagation of laser beams in the atmosphere is highly affected by aerosol scattering and atmospheric turbulence which limit the link availability on the path length. These effects are much worse than microwave relay links issue. In details, impairments are due to (i): air turbulence that caused beam spreading, beam wander, scintillation and degradation of the coherence of wave front [2], and (ii): hydrometeors (rain and snow) and suspended water particles (fog is the worst case for FSO system) that contribute to more losses due to scattering [3]. The type of scattering is determined by the size of the particles. To analyze the scattering effect, it is more suitable to utilize the geometric optics. The FSO communication link performance is measured through its availability. The tropical climate rainfall has become the major factor that affects the link availability of FSO. The link availability is estimated due to the rainfall impact.

mtkhirham@gmail.com

The attenuation due to rainfall will cause the scattering effect. The estimation is based on the rain attenuation model which correspond to the rainfall rate (mm/hr). The focus is to predict the maximum rainfall rate against the link ranges. Previous researchers have been investigating to determine the rainfall attenuation level and relating it to the rain rate [4], [5], [6], [7]. However, the scope of work focused more on European weather, and minimal effort has been channelled to investigate the work in the tropical region. Therefore, the highlight of this finding is to focus on tropical region weather condition.

In the European region, numerous findings have been conducted and the most limiting factors are found fog and snow. In tropical region with the absence of fog and snow, rain and haze are the limiting factors. Therefore, the finding of this work focuses on the impact of rainfall to the transmission of FSO communication system. Rain is chosen because it is considered the dominant weather in tropical region. The specific location chosen is Kuching, Sarawak. The rain data is officially collected from Malaysia Meteorological Department (MMD).

The study involves two approaches which are theoretical and simulation work. The theoretical approach is based on the atmospheric model which is to determine how strong the attenuation can occur in FSO communication system. The second approach is based on the simulation work utilizing the OptiSystem 7.0 to observe the effects of the attenuation to the link system. The design of parameters in the simulation involves iteration of wavelengths, size of transmitter and receiver aperture and beam divergence angle. Basically, the main objective of this finding is to get an analysis of the work based on the two approaches made. The outcome of this finding is definitely to determine on how good the transmission of FSO communication under the heavy rain weather condition. The remaining part of this paper is organized as follows. The atmospheric model and simulation setup are presented in Section 2. The results along with the discussions are made in Section 3. Section 4 obtain the conclusion of this finding.

2. MATERIAL AND METHODS

2.1 FSO Working Systems

Optical systems work in the infrared or near infrared region of light. The infrared carrier used for transmitting the signal is generated either by a high-power LED or a laser diode. Two parallel beams are used, one for transmission and one for reception, taking a standard data, voice or video signal, converting it to a digital format and transmitting it through free space [8], [9]. The beams are kept very narrow to ensure that it does not interfere with other FSO beams. The receive detectors are either PIN diodes or avalanche photodiodes. The FSO transmits invisible eye safe light beams from transmitter to the receiver using low power infrared lasers in the Tera hertz spectrum. FSO can function over kilometers [10], [11].

In FSO communication system, the medium of transmission is through the atmosphere. This will lead to the degradation of signal due to unpredictable weather condition. In this finding, rain is chosen to be the limiting factor in the performance of FSO communication system. As a result, the received signal is attenuated due to impact of rain effects, which have no fixed features. On the other hand, transmitted beam is received by the receiver lens and being transformed to an electrical source through a photodetector and preamplifier circuit on the receiving side. Hence, to obtain the transmitted data, a demodulator demodulates the electric signal. [12], [13], [14].

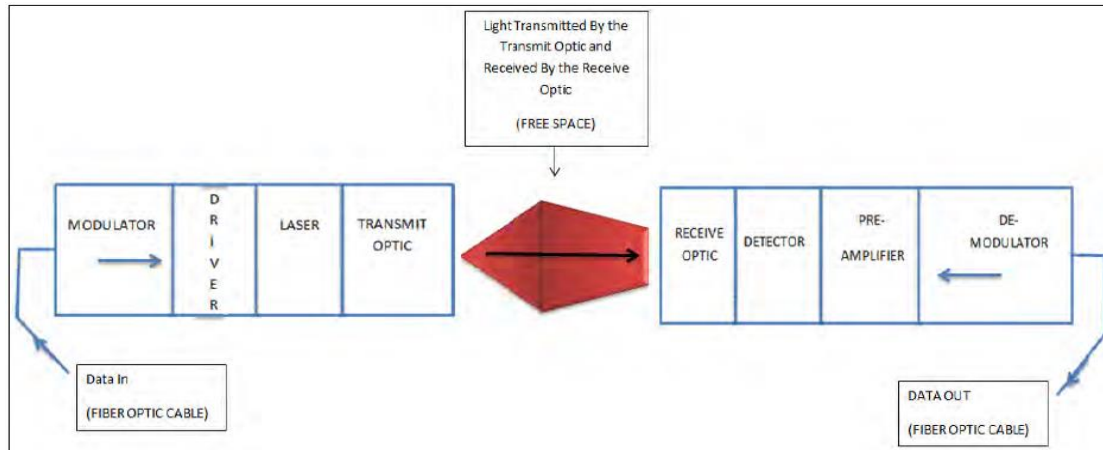


Figure 1. FSO subsystem

2.2 Rain Data

The work highlights on the impact of rain weather to the performance of FSO communication system. Hence, the data is officially provided from Malaysia Meteorological Department (MMD). The station chosen is Kuching, Sarawak as it best represents Borneo region. The data are collected based on daily readings within the period of 5 years from 2015 until 2019. The analysis concentrates on rainfall since it is the dominant weather in Borneo region. The average hourly rainfall for each month is shown in Table 1. Rainfall amount can be divided into 3 types: heavy rain (3.2mm/hour-30mm/hour), medium rain (1.6mm/hour-3.2mm/hour) and light rain (0.5mm/hour -1.6mm/hour).

Table 1 Average Rainfall Rate from January 2015 to December 2019

| Month | Heavy Rainfall (mm/hour) | Medium Rainfall (mm/hour) | Light Rainfall (mm/hour) |
|-----------|--------------------------|---------------------------|--------------------------|
| January | 5.33 | 2.19 | 0.83 |
| February | 5.28 | 2.19 | 0.88 |
| March | 4.95 | 2.18 | 0.8 |
| April | 3.48 | 2.26 | 0.95 |
| May | 0 | 2.2 | 0.81 |
| June | 3.91 | 1.83 | 1.04 |
| July | 0 | 2.53 | 0.91 |
| August | 0 | 2 | 0.9 |
| September | 0 | 1.74 | 0.86 |
| October | 3.65 | 2.27 | 0.93 |
| November | 4.63 | 2.06 | 0.85 |
| December | 5.22 | 2.22 | 0.88 |

2.3 Theoretical Approach

In theoretical approach, the main purpose is to determine the atmospheric model. There are few factors are considered in the formation of the atmospheric model. These factors are organized as follows.

2.3.1 Scattering Coefficient

Rain is precipitation droplets that condensed from atmospheric water vapour. When the droplets of rain become heavy, it will fall under gravity. Rain is under geometrical scattering where it occurs in the lower portion of the atmosphere when the particles are larger than the incident radiation. The scattering coefficient can be calculated by using Stroke Law [3].

$$\beta_{rainscat} = \pi a^2 N_a Q_{scat} \left(\frac{a}{\lambda} \right) \quad (1)$$

Where a = radius of raindrop (0.001cm to 0.1cm), N_a = rain drop distribution, Q_{scat} = scattering efficiency, λ = wavelength

2.3.2 Atmospheric Attenuation

The attenuation of laser power in the atmosphere is described by Beer's Law [15], [16].

$$\tau(R) = -\frac{P(R)}{P(O)} = e^{-(\beta)R} \quad (2)$$

Where $\tau(R)$ = transmittance at range R , $P(R)$ = laser power at R , $P(O)$ = laser power at the source, β = scattering coefficient, R = link range (km)

Equation (2) can be converted to logarithms scale using Equation (3)

$$\begin{aligned} \tau(R) &= -10 \log \frac{P(R)}{P(O)} \\ &= -10 \log e^{-\beta R} \\ &= 10 \log e^{-\beta R} \end{aligned} \quad (3)$$

2.3.3 Geometrical attenuation

Geometrical attenuation is one of the major factors that contribute loss in the atmospheric attenuation. It occurs when transmitted beam spreads with increasing of range. The beam diverges even in clear conditions and as a result, the signal power collected by the detector is lower [17]. The geometric losses are the ratio of receiver aperture surface area to the surface area of the transmit beam at the receiver.

$$Geometric Loss (GL) = \frac{\pi r_2^2}{\pi r_1^2 + \pi r_3^2} \quad (4)$$

Where r_1 = radius of transmitter aperture, r_2 = radius of receiver aperture, r_3 = radius of beam area. The geometric losses depend on the range and divergence [18].

$$Geometric Loss (GL) = \frac{\pi \left(\frac{d_2}{2} \right)^2}{\pi \left(\frac{d_1}{2} \right)^2 + \pi \left(\frac{d_3}{2} \right)^2} \quad (5)$$

Where d_1, d_2, d_3 are the diameters. Replace d_3 with θR will yield a final geometric loss expression.

$$Geometric Loss (GL) = \frac{d_2^2}{[(d_1 + (\theta R))^2]} \quad (6)$$

2.3.4 Atmospheric Model

The formation of the atmospheric model is based on the combination between atmospheric attenuation from Beer's law and the geometrical loss expression [19]. The atmospheric model equation can be written as below.

$$\frac{P_{transmit}}{P_{receive}} = 10 \log \frac{d_2^2}{[(d_1 + (\theta R))^2] \times e^{\beta R}} \quad (7)$$

Where d_2 = diameter receiver aperture (m), d_1 = diameter transmitter aperture (m), θ = beam divergence (mrad), R = link range (km), β = scattering coefficient (1/km).

2.4 FSO Simulation

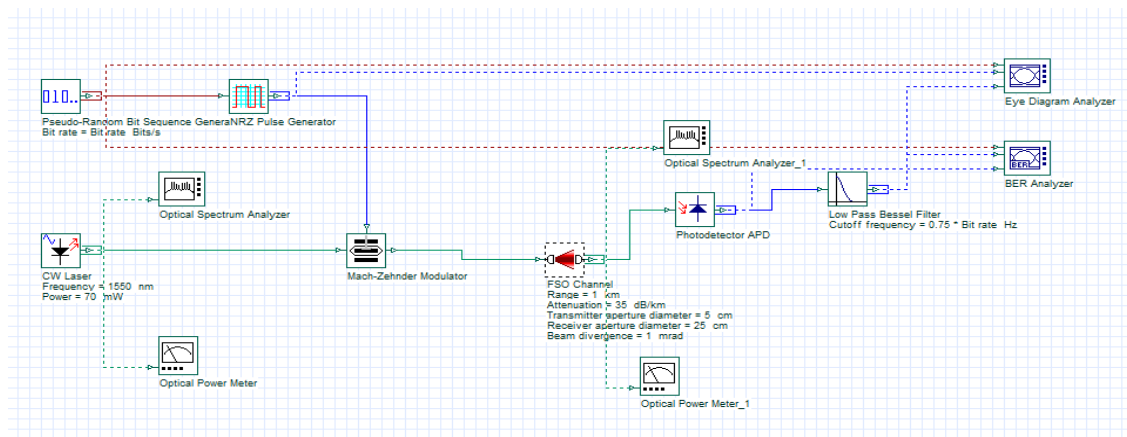


Figure 2. FSO simulation setup

2.4.1 Transmitter

Figure 2 demonstrates the simulation setup for an FSO communication device with implementation of attenuation. To generate a carrier signal, CW Laser was used in this simulation, with iteration of wavelengths at 785 nm and 1550 nm. The carrier signal was then encoded into an external Mach-Zehnder modulator for modulation process. For generating the random input data bit sequence at the rate of 155 Mbps, the pseudo-random bit sequence generator was used. In the external modulator, a non-return-to-zero (NRZ) pulse generator was set as the modulation input [20].

2.4.2 FSO Channel

The modulated data was then transmitted via the channel of the Free Space Optic (FSO). The range choice was triggered in the FSO channel and its distance was placed to be 1 km away. The attenuation considered in the connection was atmospheric effect losses (rain) ranging from low attenuations of 10 dB/km to high attenuations of 60 dB/km. Meanwhile, geometrical loss was defined in the setup by applying a transmitter aperture size of 0.05 m and a receiver aperture size of 0.25 m. The beam divergence was set to 1 mrad.

2.4.3 Receiver

The receiver side consists of a photodiode and filter. The photodiode was used for optical to electrical conversion before signal flow to a low pass filter. The decoded signal will then arrive

at signal inspection equipments such as the BER analyzer and Eye-Diagram analyzer. The received power was measured using an Optical Power Meter [21], [22].

3. RESULTS AND DISCUSSION

3.1 Theoretical Part

Figure 3 shows the performance of scattering coefficient against the rainfall intensity. The x-axis represents the rainfall rate from 0 to 6 (mm/hour). The y-axis represents the scattering coefficient in (1/km). The plotted graph is according to Equation (1).

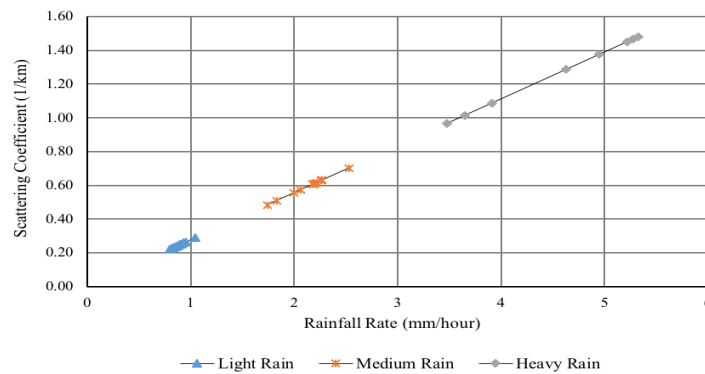


Figure 3. Scattering coefficient against rainfall rate.

The graph indicates the result of three various rain which are light, medium and heavy rain. From the graph, scattering for light rain varies from 0.22 km^{-1} to 0.29 km^{-1} while for medium rain varies from 0.48 km^{-1} to 0.70 km^{-1} and for heavy rain varies from 0.97 km^{-1} to 1.48 km^{-1} . From the analysis the heavy rain contributes higher scattering coefficient effect compared to medium and light rain. The data shows heavy rainfall rate varying from 3.48 mm/hour to 5.33 mm/hour. The graph indicates that the scattering coefficient is linearly proportional with rainfall rate. The precipitation at highest rate will contribute to a high scattering coefficient. The scattering coefficient indicates a measure of the light attenuation due to scattering of light as it traverses a medium containing scattering particles. Thus, the rise of scattering coefficient will yield high atmospheric attenuation with respect of precipitation rate and this relationship will be elaborate more and further in Figure 4.

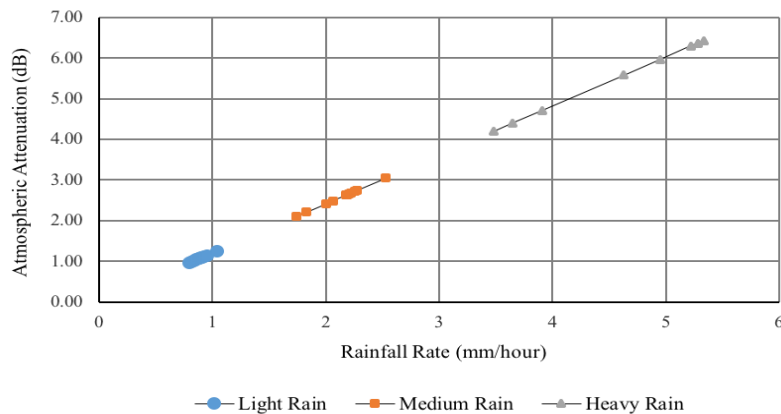


Figure 4. Atmospheric attenuation against rainfall rate

The x-axis correspond to rainfall rate and y-axis represents the atmospheric attenuation. Figure 4 proves that the atmospheric attenuation is linearly proportional with rainfall rate. The curve obtained from Equation (2) from Beer's Law [10] which explain that laser power at receiver over laser power at transmittance is equivalent with exponential scattering coefficient times link range of laser transmission. Link range between transmitter and receiver is within 1 km. As the rainfall rate increases, the attenuation will increase as well. The graph shows three different types of rain. The range of atmospheric attenuation is measure between 0.97 dB to the highest attenuation at 6.43 dB. From the graph, atmospheric attenuation for light rain varies from 0.97 dB to 1.25 dB while for medium rain varies from 2.1 dB to 3.05 dB and for heavy rain varies from 4.2 dB to 6.43 dB. As explain in Figure 3 the high scattering contributes high atmospheric attenuation. The increase in link range will also increase the atmospheric attenuation. However, this attenuation is not enough to impair the link performance.

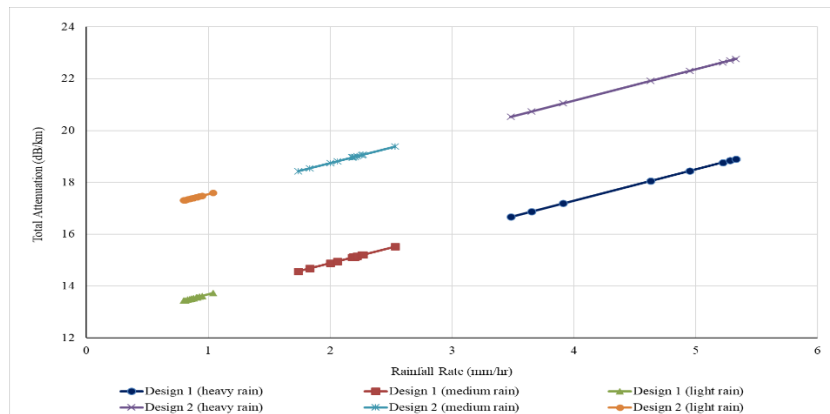


Figure 5. Total attenuation versus rainfall rate

Figure 5 illustrates the relationship between total attenuation against the rainfall rate. Note that this is based on the atmospheric model equation which involving the combination of geometric loss and atmospheric attenuation equation as well. The work consists of two different designs in terms of the transmitter and receiver aperture size. Design 1 is set to 0.05m transmitter aperture and 0.25m receiver aperture and for Design 2 both transmitter and receiver aperture are set to 0.18m. Both aperture designs are based on commercial FSO that can be found in market today. From the graph, it is clearly shows that Design 1 has better result because of the smaller size at transmitter aperture and wider at receiver aperture. This indicates that Design 1 has better characteristics in minimizing the geometrical spreading loss effect.

3.2 Simulation Part

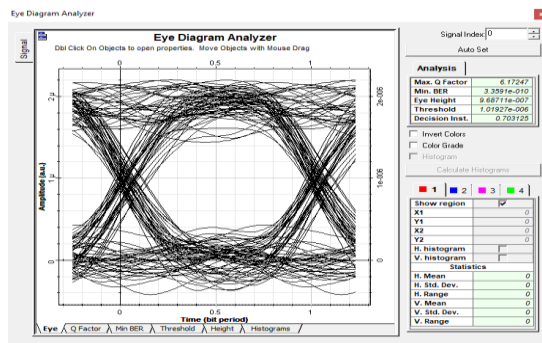


Figure 6. Eye diagram pattern for wavelength 785nm at the attenuation -35dB/km

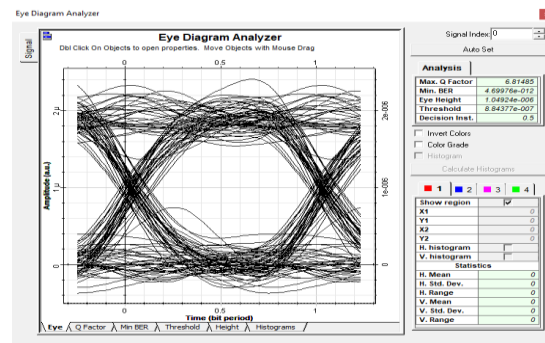


Figure 7. Eye diagram pattern for wavelength 1550nm at the attenuation -35dB/km

Figure 6 shows the eye diagrams pattern at the attenuation -35 dB/km in wavelength channel 785nm. The opening eye pattern for wavelength 785nm is small with the eye height 9.687×10^{-7} and the BER value is of the order 10^{-10} . Figure 7 shows the eye diagrams pattern at the attenuation -35 dB/km in wavelength channel 1550nm. The opening eye pattern for wavelength 1550nm is small with the eye height 1.049×10^{-6} and the BER value is of the order 10^{-12} . The wavelength with 1550nm has better BER compared to 785nm.

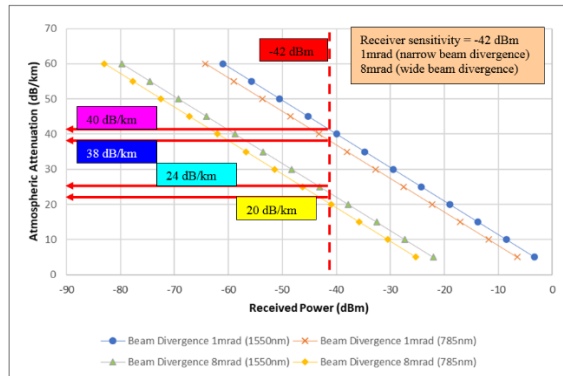


Figure 8. Received power versus attenuation for different beam divergence

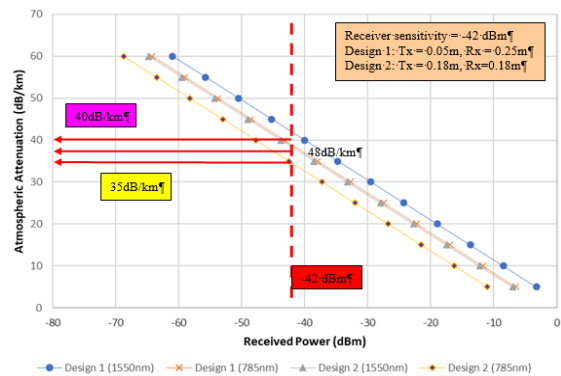


Figure 9. Received power versus attenuation for different aperture size

Figure 8 shows the comparison of beam divergence over received power due to total atmospheric effect for wavelength channel 785nm and 1550nm. It can be seen from figure that all the received power decrease constantly with the increasing of attenuation on a different beam divergence. The beam divergence at 1mrad is maximum power with the wavelength channel 1550nm. This is because the wide beam can produce bigger spot size at receiver and the possibility losing data is high due to huge power consumption. Figure 9 shows received power versus the total atmospheric attenuation for a different aperture size. The Design 1 has transmitter and receiver aperture size 0.05m and 0.25m respectively. Meanwhile Design 2 both transmitter and receiver aperture size 0.18m. All the received powers uniformly decrease when attenuation increases, and Design 1 has the maximum power with operation wavelength 1550nm. The small transmitter and large receiver for aperture size performed much better. This is because the large receiver aperture area can reduce the signal fluctuation signal by averaging the received waveform over the aperture area.

Table 2 The prediction of maximum rainfall rate at different link range

| Range (Km) | 0.5 | 1 | 1.5 | 2 | 2.5 |
|-------------------------------|---------------------------------|----|------------------|----|-----|
| Maximum Rainfall Rate (mm/hr) | 155 | 70 | 40 | 30 | 20 |
| Receiver Sensitivity | -42 dBm (APD commercially type) | | | | |
| BER=10 ⁻⁹ | | | | | |
| Aperture | Transmitter = 0.05m | | Receiver = 0.25m | | |

Table 2 shows the prediction of maximum rainfall rate at different link range FSO system. The receiver sensitivity is at bit error rate 10^{-9} and aperture selected with small transmitter and wide receiver area. It is observed that at short distance the rainfall rate is higher for the FSO system to through pass with considering receiver sensitivity. As link increases the rainfall rate will drop. This prediction rate is significant to determine the maximum range laser light able to travel and limit rainfall rate. Hence, this illustration is best describing the impact of rain attenuation to the performance of FSO communication system.

4. CONCLUSION

In this work, the research on the impact of rain upon the FSO communication system in tropical region is presented. The result shows that rain in Borneo environment can affect the transmission of FSO signal especially for severe or heavy rain condition. The simulation is based on the commercial FSO parameters. The wavelength used can optimize the line transmission with setup short distance between transmitter and receiver which can reduce the atmospheric attenuation. Hence, the usage of narrow beam is suitable and preferable for high rainfall region as it produce high power at receiver for better transmission. It also gives the advantage in data transfer rates. On the other hand, small transmitter and large receiver for aperture size performed much better. Overall, the analysis indicates that proposed FSO communication system is capable to withstand the attenuation from rain weather condition.

ACKNOWLEDGEMENTS

This research is funded by Ministry of Higher Education Malaysia under Fundamental Research Grant Scheme FRGS/1/2019/TK04/UNIMAS/02/2.

REFERENCES

- [1] A. Malik and P. Singh, "Free Space Optics: Current Applications and Future Challenges," *Int. J. Opt.* vol. **2015**, (2015) pp.1-4.
- [2] D. Anandkumar and R. G. Sangeetha, "A survey on performance enhancement in free space optical communication system through channel models and modulation techniques," *Opt. Quantum Electron*, vol **53**, (2020) pp.1-39.
- [3] U. A. Korai, L. Luini, and R. Nebuloni, "Model for the prediction of rain attenuation affecting free space optical links," *Electron.*, vol **7**, (2018) pp.1-4.
- [4] M. Achour, Simulating atmospheric free-space optical propagation: rainfall attenuation, *Free-Space Laser Communication Technologies XIV*, Proc. SPIE, vol **4635**, (2002) pp.192-201.
- [5] J.T.Ong, K.I. Timothy, Chong & S.V.B.Rao, Heavy rain effects on the propagation of free space optical links in Singapore, vol **1**, (2003) pp.365-368.
- [6] Vikas Kukshya, T.S.Rappaport, H. Izadpanah, G. Tangonan, R.A. Guerrero, J.K. Mendoza and Brey Lee, *Free-Space Optics & highspeed RF for Next Generation Networks-Propagation Measurements*, vol **1**, (2002) pp.616-620.
- [7] Haiping Wu, Hamzeh.B, Kavehrad, M, Achieving carrier class availability of FSO link via a complementary RF link, *Systems and Computers, Conference Record of the Thirty-Eighth Asilomar Conference*, vol **2**, (2004) pp.1483-1487.
- [8] A. Sangeetha, N. Sharma, and I. Deb, *J. Commun.* vol **14**, issue 3 (2019) pp.187-193.
- [9] E. Farooq, A. Sahu, and S. K. Gupta, "Survey on FSO Communication system—limitations and enhancement techniques," in *Optical and Wireless Technologies*, V. Janyani, M. Tiwari, G. Singh, and P. Minzioni, Eds. Singapore: Springer, (2018) pp.255-264.
- [10] H. Kaushal, V. K. Jain, and S. Kar, "Overview of Wireless Optical Communication Systems," in *Free Space Optical Communication*, New Delhi: Springer India, (2017) pp.1-39.
- [11] Y. Liu and H. Li, *Opt. Rev.* vol **26**, issue 3 (2019) pp.303-309.
- [12] Anuranjana, S. Kaur, and R. Goyal, 2019 6th Int. Conf. Signal Process. Integr. Networks (2019) pp.552-557.
- [13] F. K. Shaker and M. A. A. Ali, *J. Commun.* vol **14**, (2019) pp.518-523.
- [14] K. Anbarasi, C. Hemanth, and R. G. Sangeetha, *Opt. Laser Technol.* vol **97**, (2017) pp.161-171.
- [15] S. Hitam, S. N. Suhaimi, A. S. M. Noor, S. B. A. Anas, and R. K. Z. Sahbudin, "Performance analysis on 16-channels wavelength division multiplexing in free space optical

- transmission under tropical regions environment," J. Comput. Sci. vol **8**, (2012) pp.145-148.
- [16] A. Anis, A. Rahman, C. Rashidi, S. Aljunid and R. Endut, "Analysis of Atmospheric Attenuation Haze and Rainfall Effect on Free Space Optic Performance with Different Transmission Wavelength", Journal of Engineering and Applied Sciences, vol **12**, (2017) pp.4075-4079.
- [17] L W Barclay, Terahertz Propagation, Lancaster University, Book: Propagation of Radiowaves, Published (2002).
- [18] A. G. Alkholidi and K. S. Altowij, "Climate effects on performance of free space optical communication systems in Yemen," Front. Optoelectron. vol **7**, (2014) pp. 91-101.
- [19] S. A. Al-Gailani et al., "A Survey of Free Space Optics (FSO) Communication Systems, Links, and Networks," IEEE Access, vol **9**, (2021) pp.7353-7373.
- [20] R. Miglani and J. S. Malhotra, "An innovative approach for performance enhancement of 320 Gbps free space optical communication system over turbulent channel," Opt. Quantum Electron, vol **51**, (2019) pp.1-26.
- [21] V. Srivastava, A. Mandloi, and D. Patel, "Analysis of Outage Probability in Wavelength Diversity Based FSO Link Under Gamma-Gamma Fading with Varying Atmospheric Attenuation" Wirel. Pers. Commun. vol **116**, (2020) pp.1933-1947.
- [22] Anis AA, Rashidi CBM, Rahman AK, Aljunid SA, Ali N. Analysis of the effect of BER and Q-factor on free space optical communication system using diverse wavelength technique. vol **162**, (2017) pp.1-5.